

kG region, the construction of a paramagnetic resonance spectrometer at 140 GHz is difficult and expensive, but the application of this frequency by harmonic generation, with optical detection of the resonance by dichroism monitoring, is considerably simpler. It would also be interesting to study whether resonance modulation of the light will be present either in direct resonance of the F -center electron or in the hyperfine structure.^{15,16}

*Work supported by a contract from the National Science Foundation. Additional support from E. I. DuPont de Nemours & Co. is gratefully acknowledged.

†Present address: Western Electric Engineering Research Center, Princeton, N. J.

‡National Science Foundation Predoctoral Fellow.

¹G. Feher, Phys. Rev. 105, 1122 (1957).

²W. C. Holton and H. Blum, Phys. Rev. 125, 89 (1962).

³H. Seidel and H. C. Wolf, Phys. Status Solidi 11, 3 (1965).

⁴N. V. Karlev, J. Margerie, and Y. Merle d'Aubigne, J. Phys. Radium 24, 717 (1963).

⁵J. Mort, F. Lüty, and F. C. Brown, Phys. Rev. 137, A566 (1965).

⁶C. H. Henry, S. E. Schnatterly, and C. P. Slichter, Phys. Rev. 137, A583 (1965).

⁷C. H. Anderson, H. A. Weakliem, and E. A. Sabisky, Phys. Rev. 143, 223 (1966).

⁸L. F. Mollenauer, W. B. Grant, and C. D. Jeffries, Phys. Rev. Letters 20, 488 (1968).

⁹S. Geschwind, G. E. Devlin, R. L. Cohen, and S. R. Chinn, Phys. Rev. 137, A1087 (1964).

¹⁰W. T. Doyle, Phys. Rev. 131, 555 (1963).

¹¹S. N. Jasperson and S. E. Schnatterly, Bull. Am. Phys. Soc. 12, 399 (1967).

¹²S. N. Jasperson and S. E. Schnatterly, to be published.

¹³M. F. Deigen and L. B. Roitsin, Zh. Eksperim. i Teor. Fiz. 36, 176 (1959) [translation: Soviet Phys. -JETP 36, 120 (1959)].

¹⁴P. R. Moran, Phys. Rev. 135, A247 (1964).

¹⁵J. N. Dodd and G. W. Series, Proc. Roy. Soc. (London), Ser. A 263, 353 (1961).

¹⁶A. H. Firester and T. R. Carver, Phys. Rev. Letters 17, 947 (1966).

CHARGE-STATE POPULATIONS OF 5- TO 36-MeV CHANNELED OXYGEN AND CARBON IONS

F. W. Martin*

Institute of Physics, University of Aarhus, Aarhus C, Denmark

(Received 13 December 1968)

Equilibrium and nonequilibrium charge-state distributions have been obtained for high-energy ions emerging from crystals. In a major channeling direction in silicon, the slower ions and those incident in low charge states emerge nearly at equilibrium, with a mean charge close to that in a random direction. High-energy channeled oxygen 8^+ ions emerge far from equilibrium, indicating a capture cross section of less than 2×10^{-19} cm².

The fraction of particles in each state of ionization has been measured for beams of ions emerging from thin crystal foils in the direction of a major crystal axis at velocities near 10^9 cm/sec. Previous measurements have shown a decrease in the mean charge when a beam of 40-MeV iodine ions is aligned with a major axis.¹ The present results indicate a slight increase for C and O ions, together with an extremely small electron-capture cross section.

The apparatus used is the same as that for studies of electron-capture and -loss cross sections in collisions with gas atoms.² In brief, oxygen ions are accelerated in the 7-MV tandem Van de Graaff of the Niels Bohr Institute in Copenhagen and stripped to high charges in a thin carbon foil following the energy-analyzing mag-

net. Ions of a single charge are selected by a beam-switching magnet and are directed onto the thin crystal foil through a collimating system with a half-angle of acceptance 0.03° . The ions emerging from the foil pass through an aperture of half-angle $\sim 0.1^\circ$ at a scattering angle of 0 ± 0.02 and are then deflected in proportion to their charges by a third magnet. A position-sensitive detector³ and a two-dimensional pulse-height analyzer are used to obtain the number N_i of ions in each charge state i . Peak-to-valley ratios are typically greater than 10^3 , and 10^5 total counts are used, leading to a typical statistical error of 0.001 in an individual charge-state fraction Φ_i . No deadtime corrections are needed because a single electronic system is used to determine all N_i .

For the crystal experiments, a silicon surface-barrier detector is added, registering slit-edge scattering from the 1-mm-diam collimator immediately preceding the crystal. A second ion-implanted junction detector registers ions which are deflected 10° by Rutherford scattering in the crystal. In addition, the total number transmitted through the last collimator to the position-sensitive detector is counted. These numbers are designated S , R , and T , respectively. The crystals used were a 20-mm-diam silicon foil, 3400 Å thick with its $\langle 110 \rangle$ axis normal to the surface, made by etching a planar lapped slice, and a 3-mm nickel foil, ~ 1000 Å thick with its $\langle 111 \rangle$ axis normal to the surface, made by epitaxial deposition on copper deposited on mica. Both foils were self-supporting, the nickel having been chemically removed from the copper, mounted on a nickel ring, and annealed at 600°C . The crystals were held in a three-axis goniometer, accurate to 0.1° .

In a given experiment, the string direction (i.e., the crystal axis approximately normal to the surface) was aligned to within 0.1° of the beam direction, using the extreme drop in Rutherford scattering when alignment is achieved,⁴ and the major planes were located by tilting the string direction 8° to 10° from the beam direction and rotating the crystal about the direction normal to its surface.⁵ The charge-state populations Φ_i were measured (a) for beams incident in the string direction and (b) for beams incident in a random direction, defined as one some 8° from the string and not in a major plane. In addition, some scans across the string direction were made.

Figure 1 shows the results of such scans with 15.5-MeV oxygen 8^+ ions. At the bottom is the Rutherford-scattered counting rate R versus angle showing a 90% fall at the string. The half-width of this dip is 0.4° , in reasonable agreement with the theoretical critical angle $\psi_1 = 0.53^\circ$ in this case.⁶ Above this is the counting rate T in the position-sensitive detector. At angles several times the critical angle (for example at $\theta = 65^\circ$), the beam within the crystal is completely in random trajectories and is multiply scattered nearly as in an amorphous solid, with an estimated transmission less than 4% through the last collimator.⁷ When the string direction is aligned with the beam, T increases because of elimination of the usual mechanism of multiple scattering by nuclear collisions. At this point, both the

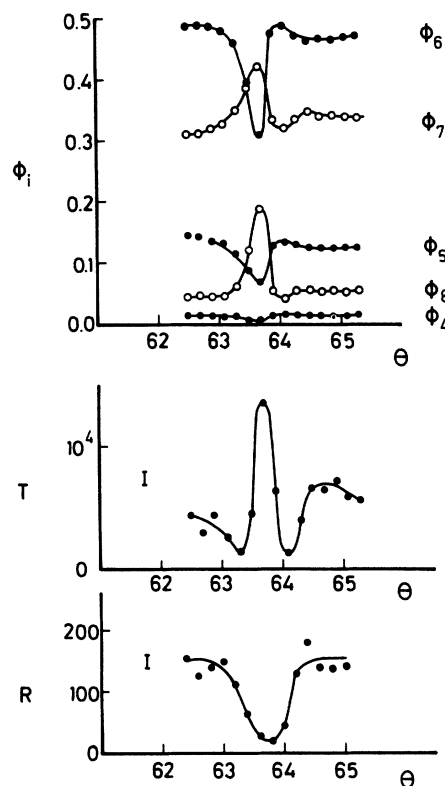


FIG. 1. Angular scan for 15.5-MeV oxygen 8^+ ions transmitted through a 3400-Å thick silicon crystal. At $\theta = 63.7^\circ$, the $\langle 110 \rangle$ direction of the crystal is aligned with the incident ion beam. The bottom curve shows the yield R of Rutherford-scattered ions for 100 slit-edge scattered counts S ; the middle curve shows the number T of transmitted particles for 20 of S ; and the top curve shows the fraction Φ_i of the transmitted ions in each charge state i .

input and output collimation apertures are well within the critical angle. The fraction of the input beam which strikes the ends of the strings and does not go into an aligned motion may be estimated as $\chi_2 \sim 0.01$ in this case,⁸ and as these particles must be strongly scattered, they contribute a negligible amount to T . Likewise, that portion of the beam is not detected which is multiply scattered out of alignment (i.e., through angles greater than ψ_1). Thus the particles transmitted at $\theta = 63.7^\circ$ must virtually all come from the aligned beam, and the charge-state fractions Φ_i shown at this angle in the top part of the figure must correspond only to aligned motion, while at $\theta = 65^\circ$, they must correspond only to random motion. Study of the best-channeled and random cases is therefore appropriate.

Table I shows the mean charges (as computed

Table I. Mean charge of random and channeled ion beams.

Crystal	Direction	Ion	Energy	Input charge	Mean charge at exit:	
					Random	Channeled
Ni	$\langle 111 \rangle$	O	35.4	8	7.10	
				7	7.09	
				6	7.07	
				5	7.10	
Ni	$\langle 111 \rangle$	C	5.2	5	4.02	4.02
				4	4.03	3.96
				3	4.02	4.02
Ni	$\langle 111 \rangle$	C	11.8	6	4.97	5.00
				5	4.96	5.00
				4	4.95	5.00
				3	4.95	5.00
Ni	$\langle 111 \rangle$	C	20.8	6	5.47	5.55
				5	5.47	5.53
				4	5.47	5.53
				3	5.47	5.53
Si	$\langle 110 \rangle$	O	8.9	8	5.36	5.46
				7	5.37	5.52
				6	5.35	5.32
				5	5.34	5.30
				4	5.36	5.30
Si	$\langle 110 \rangle$	O	15.5	8		6.71
				7	6.24	6.48
				6	6.22	6.36
				5	6.21	6.30
				4	6.24	6.29
Si	$\langle 110 \rangle$	O	15.7	8	6.12	6.88
				7	6.11	6.53
				6	6.11	6.32
				5	6.12	6.28
				4	6.13	6.25
Si	$\langle 110 \rangle$	O	24.6	8	6.74	7.42
				7	6.71	7.02
				6	6.72	6.80
				5	6.73	6.79
Si	$\langle 111 \rangle^a$	O	29.9	8	7.01	7.35
				8		7.51
Si	$\langle 110 \rangle$	O	29.9	8		7.71
				7	7.18	7.38
				6	7.17	7.10

^aIn (111) plane, $\sim 6^\circ$ from $\langle 110 \rangle$ direction.

from the values of Φ_i) for beams incident in these two directions. In the random direction, the mean charge is essentially independent of the charge state, meaning that the foil is always thick enough to establish an equilibrium charge-state distribution in this case. In the string direction, equilibrium is also obtained for carbon ions in nickel. For oxygen ions below 29.9 MeV, the weak dependence of the mean charge on the input charge for 4^+ , 5^+ , and 6^+ ions indicates that equilibrium is almost established, while the marked dependence for 7^+ and 8^+ ions indicates a nonequilibrium situation. It is apparent that the mean charge in the string direction is greater than or equal to that in the random direction for the carbon ions, which are at equilibrium, as well as for the oxygen 4^+ , 5^+ , and 6^+ ions from 15.5 to 24.6 MeV.

Since the 4^+ , 5^+ , and 6^+ ions, which are gener-

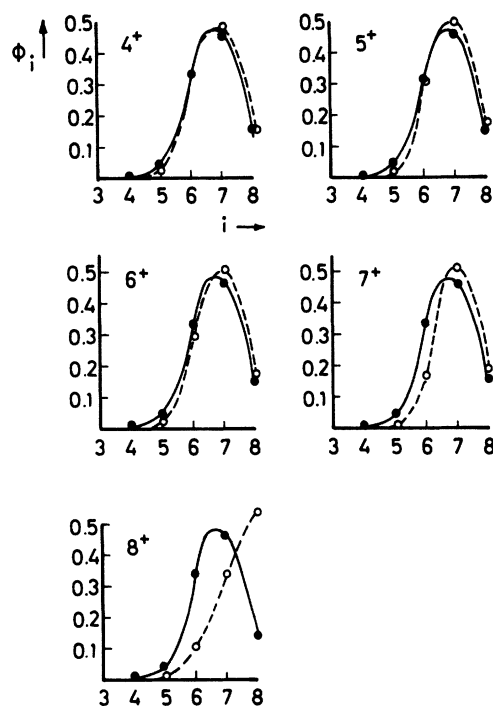


FIG. 2. Charge-state distributions for 24.6-MeV oxygen ions emerging from silicon. The dashed curves are for the aligned case and the solid curves for a random case. The charge of the incident ions is given in the upper left-hand corner of each graph.

ally below the mean charge, interact principally by electron loss and produce near-equilibrium distributions, while the 7^+ and 8^+ ions, which are generally above the mean charge, interact principally by electron capture and produce non-equilibrium distributions, one can conclude that the loss cross sections are greater than the reciprocal number of atoms/cm² in the foil, while the capture cross sections must be less. At 35.4 MeV, there is a tendency for channeled oxygen 6^+ ions to remain in charge 6, possibly indicating that the loss cross section is also approaching the reciprocal number of atoms/cm² in the foil. A similar decrease in σ_{67} above 20 MeV is seen for oxygen ions in helium gas.²

The large deviations from equilibrium for oxygen 7^+ and 8^+ ions can be seen in Fig. 2, which shows charge-state distributions for 24.6-MeV oxygen ions. In the channeled case, Φ_8 is 0.54 compared with a value of 1.00 at incidence and the equilibrium value of 0.17. The corresponding value of Φ_8 for 35.4-MeV channeled oxygen 8^+ ions is 0.76. These values indicate that the foil is thin enough for an estimate of the electron-capture cross section σ_{87} . An upper limit of 2

$\times 10^{-19}$ cm² is obtained at 35.4 MeV, using the thickness of 3400 Å calculated from the energy loss of 4-MeV oxygen ions in a random direction. This is about 100 times smaller than the value of 1.8×10^{-17} cm² for 35-MeV oxygen 8⁺ ions in argon gas.² The true value may be even smaller since a 34-Å randomly distributed oxide film could account for all the observed capture.

Small electron-capture cross sections provide an obvious explanation of the observed shift for the mean charge toward higher values in the string direction. However, the mean charge is determined by a balance between capture and loss, and a decrease in the loss cross section in the string direction has been hypothesized to explain the observed shift of the mean charge to lower values with iodine ions.⁹ The electron-loss cross section may also decrease in the string direction for oxygen and carbon ions, but there is a lower limit to this drop because of collisions with the local density of electrons in the channel. However, the electron-capture cross section may fall by a large factor for the aligned beam of oxygen ions, as may be seen by the following estimate.

An upper limit to the cross section for electron capture per electron in the crystal may be estimated as πr_c^2 , where r_c is the impact parameter at which an electron with initial velocity zero can obtain the energy $\frac{1}{2}mv^2$ in a collision with an ion of velocity v and is given by

$$r_c = 2a_0 i(v_0/v)^2,$$

in which m is the mass of the electron and $v_0 = e^2/h$.¹⁰ The actual cross section may be smaller because of prior removal of the electron¹¹ or its initial (quantum-mechanical) velocity distribution. For oxygen ions at 36 MeV, $r_c = 0.09$ Å, which is much smaller than the $\langle 110 \rangle$ channel radius of about 2.0 Å, as well as the estimated dis-

tance of closest approach to the strings $r_{\min} = 0.6$ Å for the best channeled ions.⁶ Accordingly, the oxygen ions maintain distances greater than 0.09 Å from the K and L electrons of the silicon, which are the only ones with a small prior probability of release.¹¹ The electron-capture cross section for these aligned ions should then be very much smaller than for ions in a random direction, which have close collisions with inner-shell electrons.

Thanks are due to T. C. Madden of Bell Telephone Laboratories for the silicon crystal, to F. Bason and F. Gadgaard for assistance in collecting data, to P. Ambrosius-Olesen for his painstaking efforts in fabrication of the nickel crystal, to the Niels Bohr Institute for the use of the tandem accelerator, to Dr. J. R. Macdonald for his assistance and criticism, and to Professor K. O. Nielsen for his interest in this research.

*Present address: Department of Physics and Astronomy, University of Kentucky, Lexington, Ky. 40506.

¹H. O. Lutz, S. Datz, C. D. Moak, T. S. Noggle, and L. C. Northcliffe, *Bull. Am. Phys. Soc.* **11**, 177 (1966).

²F. W. Martin and J. R. Macdonald, *Bull. Am. Phys. Soc.* **13**, 61 (1968) (to be published in more detail).

³E. Laegsgaard, F. W. Martin, and W. M. Gibson, *IEEE Trans. Nucl. Sci.* **NS-14**, 239 (1968).

⁴E. Bøgh and E. Uggerhøj, *Nucl. Instr. Methods* **38**, 216 (1965).

⁵J. U. Andersen, J. A. Davies, K. O. Nielsen, and S. L. Andersen, *Nucl. Instr. Methods* **38**, 210 (1965).

⁶J. Lindhard, *Kgl. Danske Videnskab. Selskab, Mat.-Fys. Medd.* **34**, No. 14 (1965).

⁷Ref. 6, Eqs. (4.6), (4.4), and (2.9).

⁸Ref. 6, Eq. (6.14).

⁹S. Datz, T. S. Noggle, and C. D. Moak, *Nucl. Instr. Methods* **38**, 221 (1965).

¹⁰N. Bohr, *Kgl. Danske Videnskab. Selskab, Mat.-Fys. Medd.* **18**, No. 8 (1948), Eq. (4.3.2).

¹¹N. Bohr and J. Lindhard, *Kgl. Danske Videnskab. Selskab, Mat.-Fys. Medd.* **28**, No. 7 (1954).